Relating the Electronic Structure and Reactivity of the 3d Transition Metal Monoxide Surfaces

John Kitchin, Zhongnan Xu[a], John R. Kitchin[a,*]

[a]*Department of Chemical Engineering, Carnegie Mellon University, Pittsburgh, PA 15213*

Abstract

We performed a series of density functional theory calculations of dissociative oxygen adsorption on fcc metals and their corresponding rocksalt monoxides to elucidate the relationship between the oxide electronic structure and its corresponding reactivity. We decomposed the dissociative adsorption energy of oxygen on an oxide surface into a sum of the adsorption energy on the metal and a change in adsorption energy caused by both expanding and oxidizing the lattice. We were able to identify the key features of the electronic structure that explains the trends in adsorption energies on $3d$ transition metal monoxide surfaces.

Keywords: oxide reactivity, density functional theory, transition metals, electronic structure

1. Introduction

In the past decade, the use of density functional theory (DFT) has accelerated materials discovery of new metal alloys for numerous catalysis applications [1, 2, 3, 4, 5]. One recent strategy developed to lower computational costs is to create predictive models that connect the known chemical properties of metals to the electronic structure through the use of DFT calculations [6]. This allows us to perform a coarse screening of hundreds of alloy systems for desirable properties [1, 2]. The physical accuracy of these models is based on the ability

*Corresponding author
Email address: jkitchin@andrew.cmu.edu (John R. Kitchin)

to connect the electronic structure and reactivity through simple descriptors such as the d-band width and center, which we can connect to known chemical properties of the metal [6, 7]. We propose a similar strategy should also accelerate computational materials design of metal oxides as well, but there still lacks transparent and useful electronic descriptors that have the same predictive power that the d-band center and width do for metals. However, recent work on transition metal oxides suggest these descriptors should exist. Linear scaling relationships of adsorption energies on transition metal oxides suggests that some electronic structure feature is parametric within these relationships [8, 9]. The discovery of simple electron counting rules for adsorption energies on oxides also suggest a hidden electronic structure correlation [10]. Finally, a few studies have been able to directly relate properties of the oxygen p-band [11, 12] and bulk transition metal e_g and d-band to reactivity on perovskites [13, 14].

To understand relationships between oxide electronic structure and their reactivities, we draw our inspiration from a seminal paper by Gelatt et al. on the theory of bonding of transition metals to non-transition metals [15] and a recent DFT paper that validated these results for metal rutile dioxides [16]. They recognized that there were two primary steps to transform a bulk transition metal into a compound with a non-transition metal: lattice expansion of the transition metal and then subsequent bonding with the non-transition metal. They were able to describe the formation energy of the compound as a sum of an energy cost of expansion and an energy gain of making bonds between the transition metal and non-transition metal. Finally, they connected physical and electronic structure properties to explain formation energy trends. We propose a similar approach to understand the relationship between the electronic structure and reactivity on oxide surfaces.

In this work, we elucidate the relationship between the reactivity and electronic structure of oxides by using structural perturbations to connect the reactivity of an oxide surface with that of a metal. We chose to perform this analysis on six first row transition metals (Ti, V, Mn, Co, Ni, Cu) constrained to the fcc

structure and their corresponding rocksalt monoxides (TiO, VO, MnO, CoO, NiO, CuO). We recognized that there were two simple structural perturbations between the fcc and rocksalt structure: isotropic expansion and an insertion of an interpenetrating oxygen fcc lattice. The intermediate structure then is the expanded metal fcc lattice that has the same lattice constant as its respective oxide. By calculating adsorption energies on the metal, expanded metal, and oxide, we can decompose the adsorption energies on the monoxide as a sum of the adsorption energy on the metal and the change in the adsorption energy caused by both expanding and oxidizing the metal lattice. We can then connect changes in the structure and composition of the surface to changes in the electronic structure, which we ultimately relate to the reactivity. To interpret reactivities from the electronic structure, we first found that adsorption energy on both metals and oxides have the same correlation with the oxygen p-band center. We then found that expansion of the lattice causes either a narrowing or a complete breakdown of the d-band that typically leads to a weaker surface-adsorbate bond, and oxidation of the lattice produces a downward shift in the surface d-band which can result in stronger adsorption if the surface d-bands and adsorbate p-bands are degenerate in energy. These conclusions shed new insight into not only possible electronic descriptors but also their physical origins.

2. Methods

A complete log of the bulk calculations and their corresponding discussion can be found in the supporting information. Briefly, all calculations were performed with the Vienna Ab-initio Simulation Package (VASP) [17, 18]. The core electrons were described by the projector-augmented wave (PAW) method [19, 20] and the exchange correlation functional used was the Perdew-Burke-Ernzerhof (PBE) [21, 22] generalized gradient approximation (GGA). The Kohn-Sham orbitals were expanded with plane-waves up to a 520 eV cutoff. All k-points were represented on Monkhorst-Pack grids [23]. For bulk calculations,

an 8 8 8 grid k-point grid was used for metals and a 7 7 7 for the expanded metals and oxides. Calculations of adsorption energies on all surfaces were done with a 7 7 1 k-point grid with 10 Å of vacuum, and the density of states (DOS) analysis on surfaces were done with a higher (12 12 1) k-point grid to ensure a fine quality DOS. Surface d and p band centers (E_d) were done via the first moment of the projected DOS about the Fermi level (E_f) and is expressed as

$$E_d = \frac{\int \rho E dE}{\int \rho dE} \tag{1}$$

All bulk and slab calculations were done including spin-polarization in both ferromagnetic and antiferromagnetic states (see supporting information). The lattice constants used for slab construction were determined from the bulk calculations. Slab calculations were done with symmetric cells with six metal layers. The middle two layers were held at fixed positions, while the outer four layers (two for each side) were allowed to relax in the direction perpendicular to the surface. For calculations including relaxation, the force criteria was set to 0.05 eV/Å. Images of the bulk and surface structures as well as the adsorption sites can be seen in Figure 1. The adsorption energies normalized per O atom are calculated according to this equation:

$$E$$

$$_{ads}(\text{eV/O}) = 1_{\overline{2(E}\,slab,O_2}\text{ - (E}_{slab}\text{ + E}_{O_2}\text{))} \tag{2}$$

In Equation 2, E_{slab,O_2} and E_{slab} are total energies of the symmetric slab with and without an O atom adsorbate on both sides, while E_{O_2} is the total energy of an oxygen molecule calculated in an asymmetric box. The 1.36 eV correction for the overbinding energy of the oxygen molecule found by Wang *et al.* was used [24].

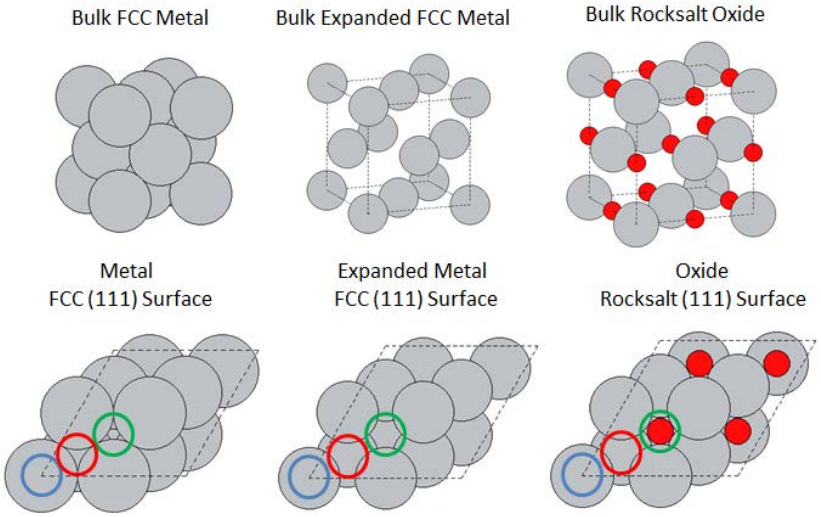

Figure 1: Shows the structural transformations to go from an FCC metal to a rocksalt oxide. We also show the corresponding surface transformations on equivalent surfaces of the two materials. Blue, green, and red circles show the top, fcc, and hcp, respectively, adsorption sites used in this study.

3. Results and Discussion

We first performed calculations on the bulk unit cells to find the equilibrium lattice constants and most stable magnetic ordering for metals and oxides. We then used the equilibrium structures and stable magnetic orderings to calculate adsorption energies on metal and oxide surfaces on the top, fcc, and hcp adsorption sites. From Figure 2a, we see that, in general, the adsorption trends on oxides and metals on the different adsorption sites are similar. As the number of d-electrons increases, the adsorption energies decrease, which is consistent with a number of previous works that looked at trends in adsorption energies across first row transition metal oxides [10, 14].

To understand the contributions to the trends in the adsorption energies on the oxides, we calculated adsorption energies on an intermediate structure: the expanded fcc metal lattice. This expanded lattice has the same volume per metal atom as the oxide but lacks the lattice oxygen. To study the change in the

bonding between the adsorbate and this artificially expanded lattice, only the adsorbate was allowed to relax in these adsorption calculations. By calculating adsorption energies on this structure, we show how the adsorption energy on the oxide is a sum of the original metal adsorption energy, a change in the adsorption energy caused by expanding the metal lattice, and a change in the adsorption energy caused by oxidizing the expanded lattice. For the rest of the paper we will refer to these changes in the adsorption energy as the "expansion energy" and the "oxidation energy". Figures 2b-d show that the trends in expansion and oxidation energies are consistent across the different adsorption sites, and that the expansion energy is generally positive (weakens the surface-adsorbate bond) and the oxidation energy is generally negative (strengthens the surface-adsorbate bond). The magnitude of both energies rises as one goes from the beginning to the middle of the first row transition metals and then decreases going to the late first row transition metals.

The primary value of doing the calculations on the expanded metal lattice is that it allows us to systematically connect changes in the atomic structure and composition to changes in the electronic structure, which we ultimately need to relate to the adsorption energy. However, we first need a way to interpret changes in the electronic structure to changes in the adsorption energy. To do this, we fall back to the original d-band model, which related the position of the adsorbate bonding and anti-bonding states (in our case the oxygen p-states) to the position of the center and width of the d-band [25]. These original results suggest that one way to interpret changes in the adsorption energies is by directly looking at the average energy of the adsorbate states. We first show this method is valid for metals and consistent with the d-band model in Figure 3a. Furthermore, in Figure 3b, we show the position of the adsorbate p-states can also be used to understand the adsorption energies of not only the metals, but also the expanded metals and oxides as well. The fact that the same electronic structure correlation can be used for both metals and oxides is quite extraordinary and suggests similar bonding mechanisms on both surfaces. We note that the outliers are the adsorption energies on expanded manganese and

cobalt. The reason for these outliers is that the manganese and cobalt expanded lattice is so large that the nature of the adsorbate surface bond resembles more individual molecular bonds, and our simple calculation of the average p-state energy is insufficient to capture the reactivity.

Now that we are able to correlate the electronic structure with the adsorption energy on all surfaces, the next step is to interpret the relationship between changes in the atomic structure and composition going from a metal to an oxide (expansion and oxidation) to changes in the adsorption energy. The starting point of our analysis is adsorption on metals, which is easily understood through the original d-band model, and this is seen in the figures of the surface atom projected, electronic structure of early (Ti), mid (Mn), and late (Cu) transition metals with an adsorbate on the fcc site (Figures 4a, c, and e). In Figure 4b, d, and f, we see that expanding the lattice produces changes in the d-band that shift the position of the oxygen p-band. On early transition metals (Figure 4a, b), expanding the lattice narrows the d-band and produces a down shift of the d-band center, which raises (weakens) the adsorption energy. These results are consistent with past studies that calculated strain induced changes in the adsorption energy on early transition metals [26]. For mid transition metals (Figure 4c, d), the expansion of the lattice is so large that the d-band splits into bonding and anti-bonding parts. The large increases in the adsorption energy are associated with a high amount of tensile strain (26% for Mn) and a lack of hybridization between surface d-states and adsorbate p-states. On late transition metals (Figure 4e, f) expansion of the lattice also narrows the d-band, but has opposite effects on the adsorption energy between Ni and Cu. The effect of strain on the adsorption on late transition metals has previously been explored in numerous articles, and the main conclusion is that narrowing of the d-band produces a shift down in energy, which decreases (strengthens) the adsorption energy, which is consistent with our result on Ni and inconsistent with our result on Cu [27]. To explain this discrepancy, we note that the tensile strain we apply on Ni and Cu are 19% and 17%, which is up to four times higher than the tensile strain used in past studies on Cu [27]. Similar to mid

transition metals, it is apparent that the high amount of tensile strain pushes up the adsorbate p-band bonding states to higher energies and also lowers the amount of hybridization between the surface d-band and adsorbate p-states, both of which would result in a weaker bond and higher adsorption energy.

Following expansion, the lattice goes through oxidation, which is an insertion of an interpenetrating fcc oxygen lattice and the formation of six metal-oxygen bonds per metal. This bonding is apparent through the hybridization of the lattice oxygen p-states with the metal d-states to create hybridized states at lower energies (Figure 5). The position of these new hybridized states indicates how much energy can be gained by an oxygen bonding to an under-coordinated surface. In addition, the adsorbate bonding states are shifted up in energy with respect to their energies on the expanded lattice. We observed that whenever the energy of the adsorbate bonding states on the expanded lattice are degenerate in energy with the new hybridized lattice metal-oxygen states, the surface-adsorbate bond is strengthened through additional hybridization between adsorbate p-states and surface d-states. This is most prominent for mid (Figure 5c, d) and late transition metal oxides (Figure 5e, f). Furthermore, as one goes from mid to late transition metal oxides, these new hybridized bonding states move up in energy, thereby lowering the amount the surface-adsorbate bond can be strengthened through oxidizing the lattice. In contrast to mid and late transition metal oxides, the early transition metal oxide hybridized states are deeper in energy than the adsorbate bonding states, which led to little hybridization between the adsorbate bonding states and surface states (Figures 5a, b). The lack of hybridization in addition to the upshift in energy of the adsorbate states led to an overall increase (weakening) of the adsorption energy on early transition metal oxides.

4. Conclusions

We identified key features of oxide electronic structure that determine the strength of the dissociative adsorption energy of oxygen. We did this by per-

forming structural perturbations to transform a fcc metal into a rocksalt monoxide, tracking changes in both the adsorption energy and electronic structure and how they relate to changes in the surface atomic structure and composition. We found that expanding the metal lattice narrowed and produced shifts in the d-band, and the effect on the adsorption energy depended on both the magnitude of the volume expansion and the position of the metal on the periodic table. We also found that oxidizing the lattice allows the surface to form stronger bonds with the adsorbate if the energies of the bulk bonding d-band states created through hybridization with bulk oxygen p-states are degenerate with the adsorbate p-band states. The position of the bulk bonding d-states formed through oxidizing the lattice also determines the strength of this effect. To interpret these relationships between the electronic structure and adsorption energy, we found a common correlation between the energies of the adsorbate p-bands and adsorption energy for both metals and oxides. These results elucidate the mechanism of adsorption and provide insight into the relationship between electronic structure and reactivity on oxide surfaces.

Acknowledgement

We gratefully acknowledge support from the DOE Office of Science Early Career Research program (DE-SC0004031).

References

[1] N. Ínoğlu, J. R. Kitchin, Identification of sulfur-tolerant bimetallic surfaces using dft parametrized models and atomistic thermodynamics, ACS Catalysis 1 (4) (2011) 399–407. arXiv:http://pubs.acs.org/doi/pdf/10.1021/cs200039t, doi:10.1021/cs200039t.
URL `http://pubs.acs.org/doi/abs/10.1021/cs200039t`

[2] H. Xin, A. Holewinski, S. Linic, Predictive structurereactivity models for rapid screening of pt-based multimetallic electrocata-

lysts for the oxygen reduction reaction, ACS Catalysis 2 (1) (2012) 12–16. arXiv:http://pubs.acs.org/doi/pdf/10.1021/cs200462f, doi:10.1021/cs200462f.
URL http://pubs.acs.org/doi/abs/10.1021/cs200462f

[3] J. Greeley, T. F. Jaramillo, J. Bonde, I. B. Chorkendorff, J. K. Nrskov, Computational high-throughput screening of electrocatalytic materials for hydrogen evolution., Nature Materials 5 (11) (2006) 909–13. doi:10.1038/nmat1752.
URL http://www.nature.com/nmat/journal/v5/n11/abs/nmat1752.html

[4] M. P. Andersson, T. Bligaard, A. Kustov, K. E. Larsen, J. Greeley, T. Johannessen, C. H. Christensen, J. K. Nrskov, Toward computational screening in heterogeneous catalysis: Pareto-optimal methanation catalysts, Journal of Catalysis 239 (2) (2006) 501 – 506. doi:http://dx.doi.org/10.1016/j.jcat.2006.02.016.
URL http://www.sciencedirect.com/science/article/pii/S0021951706000674

[5] C. J. H. Jacobsen, S. Dahl, B. S. Clausen, S. Bahn, A. Logadottir, J. K. Nørskov, Catalyst design by interpolation in the periodic table: Bimetallic ammonia synthesis catalysts, Journal of the American Chemical Society 123 (34) (2001) 8404–8405, pMID: 11516293. arXiv:http://pubs.acs.org/doi/pdf/10.1021/ja010963d, doi:10.1021/ja010963d.

[6] N. nolu, J. R. Kitchin, New solid-state table: estimating d-band characteristics for transition metal atoms, Molecular Simulation 36 (7-8) (2010) 633–638. arXiv:http://www.tandfonline.com/doi/pdf/10.1080/08927022.2010.481794, doi:10.1080/08927022.2010.481794.
URL http://www.tandfonline.com/doi/abs/10.1080/08927022.2010.481794

[7] J. R. Kitchin, J. K. Nørskov, M. A. Barteau, J. G. Chen, Role of strain and ligand effects in the modification of the electronic and chem-

ical properties of bimetallic surfaces, Phys. Rev. Lett. 93 (2004) 156801. doi:10.1103/PhysRevLett.93.156801.
URL http://link.aps.org/doi/10.1103/PhysRevLett.93.156801

[8] E. Fernndez, P. Moses, A. Toftelund, H. Hansen, J. Martnez, F. Abild-Pedersen, J. Kleis, B. Hinnemann, J. Rossmeisl, T. Bligaard, J. Nrskov, Scaling relationships for adsorption energies on transition metal oxide, sulfide, and nitride surfaces, Angewandte Chemie International Edition 47 (25) (2008) 4683–4686. doi:10.1002/anie.200705739.
URL http://dx.doi.org/10.1002/anie.200705739

[9] I. C. Man, H.-Y. Su, F. Calle-Vallejo, H. A. Hansen, J. I. Martnez, N. G. Inoglu, J. Kitchin, T. F. Jaramillo, J. K. Nrskov, J. Rossmeisl, Universality in Oxygen Evolution Electrocatalysis on Oxide Surfaces, ChemCatChem 3 (7) (2011) 1159–1165. doi:10.1002/cctc.201000397.
URL http://doi.wiley.com/10.1002/cctc.201000397

[10] F. Calle-Vallejo, N. G. Inoglu, H.-Y. Su, J. I. Martinez, I. C. Man, M. T. M. Koper, J. R. Kitchin, J. Rossmeisl, Number of outer electrons as descriptor for adsorption processes on transition metals and their oxides, Chem. Sci. 4 (2013) 1245–1249. doi:10.1039/C2SC21601A.
URL http://dx.doi.org/10.1039/C2SC21601A

[11] Y.-L. Lee, J. Kleis, J. Rossmeisl, Y. Shao-Horn, D. Morgan, Prediction of solid oxide fuel cell cathode activity with first-principles descriptors, Energy Environ. Sci. 4 (2011) 3966–3970. doi:10.1039/C1EE02032C.
URL http://dx.doi.org/10.1039/C1EE02032C

[12] J. Suntivich, K. J. May, H. A. Gasteiger, J. B. Goodenough, Y. Shao-Horn, A perovskite oxide optimized for oxygen evolution catalysis from molecular orbital principles, Science 334 (6061) (2011) 1383–1385. arXiv:http://www.sciencemag.org/content/334/6061/1383.full.pdf, doi:10.1126/science.1212858.
URL http://www.sciencemag.org/content/334/6061/1383.abstract

[13] S. A. Akhade, J. R. Kitchin, Effects of strain, d-band filling, and oxidation state on the bulk electronic structure of cubic 3d perovskites, The Journal of Chemical Physics 135 (10) (2011) 104702. doi:10.1063/1.3631948.
URL http://link.aip.org/link/?JCP/135/104702/1

[14] S. A. Akhade, J. R. Kitchin, Effects of strain, d-band filling, and oxidation state on the surface electronic structure and reactivity of 3d perovskite surfaces, The Journal of Chemical Physics 137 (8) (2012) 084703. doi:10.1063/1.4746117.
URL http://link.aip.org/link/?JCP/137/084703/1

[15] C. D. Gelatt, A. R. Williams, V. L. Moruzzi, Theory of bonding of transition metals to nontransition metals, Phys. Rev. B 27 (1983) 2005–2013. doi:10.1103/PhysRevB.27.2005.
URL http://link.aps.org/doi/10.1103/PhysRevB.27.2005

[16] J. I. Martínez, H. A. Hansen, J. Rossmeisl, J. K. Nørskov, Formation energies of rutile metal dioxides using density functional theory, Phys. Rev. B 79 (2009) 045120. doi:10.1103/PhysRevB.79.045120.
URL http://link.aps.org/doi/10.1103/PhysRevB.79.045120

[17] G. Kresse, J. Furthmüller, Efficient iterative schemes for *ab initio* total-energy calculations using a plane-wave basis set, Phys. Rev. B 54 (1996) 11169–11186. doi:10.1103/PhysRevB.54.11169.
URL http://link.aps.org/doi/10.1103/PhysRevB.54.11169

[18] G. Kresse, J. Furthmller, Efficiency of ab-initio total energy calculations for metals and semiconductors using a plane-wave basis set, Computational Materials Science 6 (1) (1996) 15 – 50. doi:http://dx.doi.org/10.1016/0927-0256(96)00008-0.
URL http://www.sciencedirect.com/science/article/pii/0927025696000080

[19] P. E. Blöchl, Projector augmented-wave method, Phys. Rev. B 50 (1994) 17953–17979. doi:10.1103/PhysRevB.50.17953.
URL http://link.aps.org/doi/10.1103/PhysRevB.50.17953

[20] G. Kresse, D. Joubert, From ultrasoft pseudopotentials to the projector augmented-wave method, Phys. Rev. B 59 (1999) 1758–1775. doi:10.1103/PhysRevB.59.1758.
URL http://link.aps.org/doi/10.1103/PhysRevB.59.1758

[21] J. P. Perdew, K. Burke, M. Ernzerhof, Generalized gradient approximation made simple, Phys. Rev. Lett. 77 (1996) 3865–3868. doi:10.1103/PhysRevLett.77.3865.
URL http://link.aps.org/doi/10.1103/PhysRevLett.77.3865

[22] J. P. Perdew, K. Burke, M. Ernzerhof, Generalized gradient approximation made simple, Phys. Rev. Lett. 78 (1997) 1396–1396. doi:10.1103/PhysRevLett.78.1396.
URL http://link.aps.org/doi/10.1103/PhysRevLett.78.1396

[23] H. J. Monkhorst, J. D. Pack, Special points for brillouin-zone integrations, Phys. Rev. B 13 (1976) 5188–5192. doi:10.1103/PhysRevB.13.5188.
URL http://link.aps.org/doi/10.1103/PhysRevB.13.5188

[24] L. Wang, T. Maxisch, G. Ceder, Oxidation energies of transition metal oxides within the GGA + U framework, Physical Review B 73 (19) (2006) 195107.

[25] B. Hammer, J. K. Nrskov, Why gold is the noblest of all the metals, Nature 376 (6537) (1995) 238–240. doi:10.1038/376238a0.
URL http://www.nature.com/doifinder/10.1038/376238a0

[26] S. Schnur, A. Groß, Strain and coordination effects in the adsorption properties of early transition metals: A density-functional theory study, Phys. Rev. B 81 (2010) 033402. doi:10.1103/PhysRevB.81.033402.
URL http://link.aps.org/doi/10.1103/PhysRevB.81.033402

[27] M. Mavrikakis, B. Hammer, J. K. Nørskov, Effect of strain on the reactivity of metal surfaces, Phys. Rev. Lett. 81 (1998) 2819–2822.

doi:10.1103/PhysRevLett.81.2819.

URL http://link.aps.org/doi/10.1103/PhysRevLett.81.2819

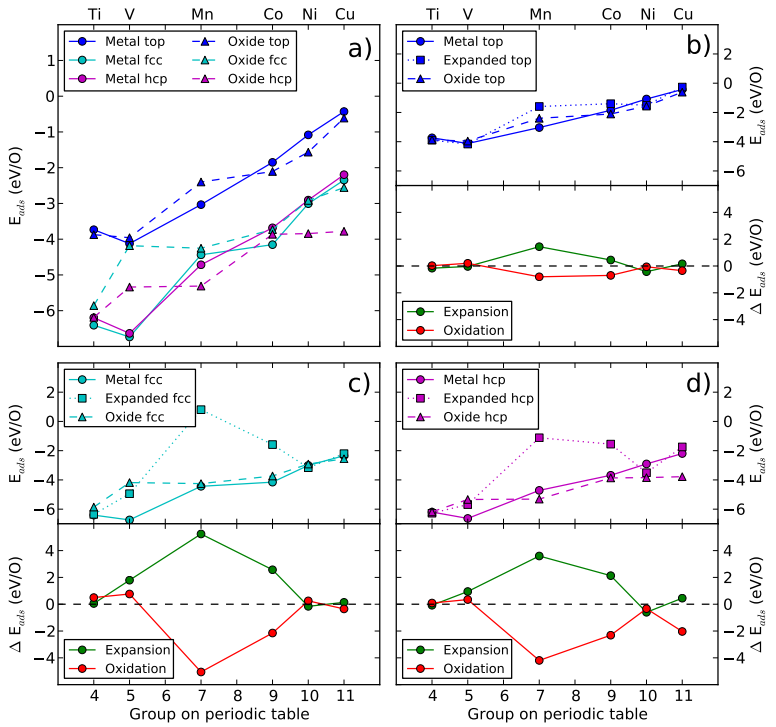

Figure 2: a) shows the adsorption energies on metals and oxides on all the sites. b), c), and d) show the contributions of expansion energy and oxidation energy to the adsorption energies on oxides. The expansion energy is the change in the adsorption energy caused by expanding the metal, while the oxidation energy is the change in the adsorption energy caused by oxidizing the expanded metal. The top halves of b), c), and d) show the absolute adsorption energies on the metal, metal with the expanded lattice, and oxide, while the bottom halves show the change in adsorption energy caused by lattice expansion (green) and by lattice oxidation (red).

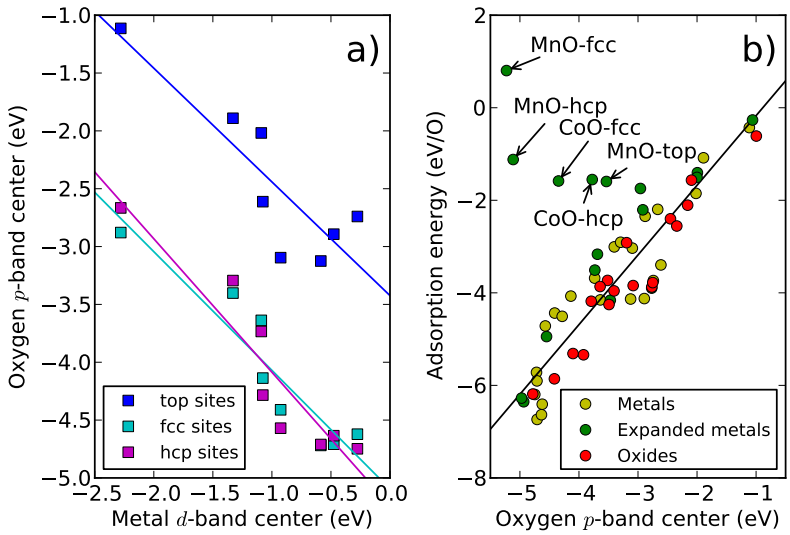

Figure 3: a) shows the correlation between the surface projected d-band center and the average energy of the adsorbate p-states on the top, fcc, and hcp adsorption sites on metals. b) shows the correlation between the adsorption energy and the average energy of the adsorbate p-states on metals, expanded metals, and oxides on all sites.

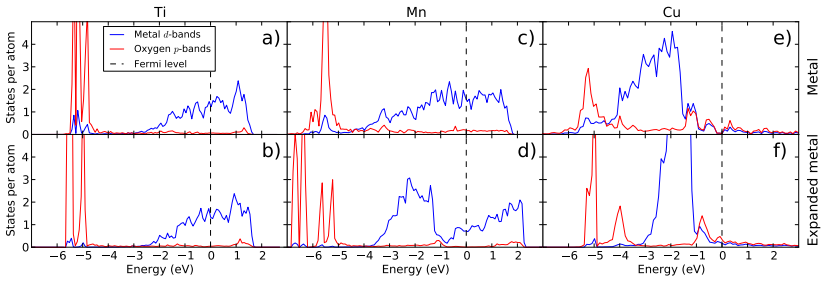

Figure 4: a) and b) show the density of states of Ti and expanded Ti with oxygen adsorbed at the fcc site. c) and d) show the density of states of Mn and expanded Mn with oxygen adsorbed at the fcc site. e) and f) show the density of states of Cu and expanded Cu with oxygen adsorbed at the fcc site.

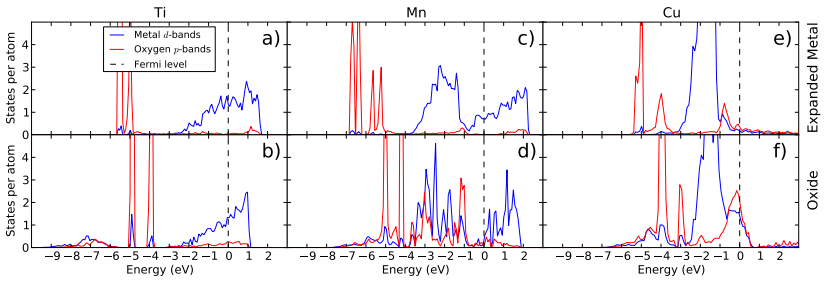

Figure 5: a) and b) show the density of states of expanded Ti and TiO with oxygen adsorbed at the fcc site. c) and d) show the density of states of expanded Mn and MnO with oxygen adsorbed at the fcc site. e) and f) show the density of states of expanded Cu and CuO with oxygen adsorbed at the fcc site.